

Response of CO₂ and H₂O fluxes of a mountainous tropical rainforest in equatorial Indonesia to El Niño events

A. Olchev^{1,2}, A. Ibrom³, O. Panferov⁴, D. Gushchina⁵, H. Kreilein², V. Popov^{6,7}, P. Propastin², T. June⁸, A. Rauf⁹, G. Gravenhorst* and A. Knohl²

[1] {A.N. Severtsov Institute of Ecology and Evolution of RAS, Moscow, Russia}

[2] {Department of Bioclimatology, Faculty of Forest Sciences and Forest Ecology, Georg-August University of Goettingen, Goettingen, Germany}

[3] {Department for Environmental Engineering, Technical University of Denmark, Kgs. Lyngby, Denmark}

[4] {Climatology and Climate Protection, Faculty of Life Sciences and Engineering, University of Applied Sciences, Bingen am Rhein, Germany}

[5] {Department of Meteorology and Climatology, Faculty of Geography, Moscow State University, Moscow, Russia}

[6] {Faculty of Physics, Lomonosov Moscow State University, Moscow, Russia}

[7] {Financial University under the Government of the Russian Federation, Moscow, Russia}

[8] {Bogor Agricultural University, Department of Geophysics and Meteorology}

[9] {Universitas Tadulako, Palu, Indonesia}

[*] {Retired}

Correspondence to: A. Olchev (aoltche@gmail.com)

Abstract

The possible impact of El Niño-Southern Oscillation (ENSO) events on the main components of CO₂ and H₂O fluxes between tropical rainforest and atmosphere is investigated. The fluxes were continuously measured in a old-growth mountainous tropical rainforest growing in Central Sulawesi in Indonesia using the eddy covariance method for the period from January 2004 to June 2008. During this period, two episodes of El Niño and one episode of La Niña were observed. All these ENSO episodes had moderate intensity and were of Central Pacific type. The temporal variability analysis of the main meteorological parameters and components of CO₂ and H₂O exchange showed a high sensitivity of Evapotranspiration (ET) and Gross Primary Production (GPP) of the tropical rainforest to meteorological variations caused by both El Niño and La Niña episodes. Incoming solar radiation is the main governing factor that is responsible for ET and GPP

1 variability. Ecosystem Respiration (RE) dynamics depend mainly on the air temperature changes
2 and are almost insensitive to ENSO. Changes of precipitation due to moderate ENSO events did not
3 cause any notable effect on ET and GPP, mainly because of sufficient soil moisture conditions even
4 in periods of anomalous reduction of precipitation in the region.

6 **1. Introduction**

7 The contribution of tropical rainforests to the global budget of greenhouse gases, their
8 possible impact on the climatic system, and their sensitivity to climatic changes are key topics of
9 numerous theoretical and experimental studies (Clark and Clark, 1994; Grace et al., 1995, 1996;
10 Malhi et al., 1999; Ciais et al., 2009; Lewis et al., 2009; Phillips et al., 2009; Malhi, 2010; Fisher et
11 al., 2013; Moser et al., 2014). The area covered by tropical rainforests was drastically reduced
12 during the last century, mainly due to human activities and presently there are less than 11.0 million
13 km² remaining (Malhi, 2010). While deforestation rates in the tropical forests of Brazil are now
14 declining, countries in South-East Asia, particularly Indonesia, show globally the largest increase in
15 forest loss (Hansen et al., 2013), resulting in major changes in carbon and water fluxes between the
16 land surface and the atmosphere. Therefore, during the last decade the tropical forest ecosystems of
17 South-East Asia and especially Indonesia are the focus area of intensive studies of biogeochemical
18 cycle and land surface - atmosphere interactions. On the one hand, it is necessary to know how
19 these tropical forests influence the global and regional climate, and on the other hand, how they
20 respond to changes of regional climatic conditions.

21 Climate and weather conditions in the equatorial Pacific and South-Eastern part of Asia are
22 mainly influenced by the Intertropical Convergence Zone (ITCZ) which is seasonally positioned
23 north and south of the equator. Another very important factor affecting the climate of South-East
24 Asia is the well-known coupled oceanic and atmospheric phenomenon, El Niño-Southern
25 Oscillation (ENSO). During the warm phase of ENSO, termed "El Niño", sea surface temperature
26 (SST) in the central and eastern parts of the equatorial Pacific sharply increases, and during a cold
27 phase of the phenomenon, termed "La Niña", the SST in these areas is lower than usual. Both
28 phenomena, El Niño and La Niña, lead to essential changes of pressure distribution and atmospheric
29 circulation and, as a result, to anomalous changes of precipitation amount, solar radiation, and
30 temperature fields, both in the regions of sea surface temperature anomalies and in a wide range of
31 remote areas through the mechanism of atmospheric bridges (Wang, 2002; Graf and Zanchettin,
32 2012, Yuan and Yan, 2013). Typically, in Indonesia El Niño results in dryer conditions and La Niña
33 results in wetter conditions, potentially impacting the land vegetation (Erasmí et al., 2009). ENSO

1 events are irregular, characterised by different intensity and, are usually observed at intervals of 2-7
2 years.

3 To describe the possible effects of ENSO events on CO₂ and H₂O exchange between land
4 surface and the atmosphere, many studies for different Western Pacific regions were carried out
5 during the recent decades (Feely et al., 1998; Malhi et al., 1999; Rayner and Law, 1999; Aiba and
6 Kitayama, 2002; Hirano et al., 2007; Erasmi et al., 2008; Gerold and Leemhuis, 2010). They are
7 mainly based on the results of modelling experiments and remote sensing data (Rayner and Law,
8 1999). Experimental results based on direct measurements of CO₂ and H₂O fluxes, which allow
9 studying the response of individual terrestrial ecosystems to anomalous weather conditions, are still
10 very limited (e.g. Hirano et al., 2007; Moser et al., 2014). Existing monitoring networks in
11 equatorial regions of the Western Pacific are associated mainly with lowland areas and do not cover
12 mountainous rainforest regions, even though mountainous regions cover some of the last remaining
13 undisturbed rainforest in South-East Asia. Most attention in former studies was paid to the
14 description of plant response to anomalously dry and warm weather during El Niño events (Aiba
15 and Kitayama, 2002; Hirano et al., 2007; Moser et al., 2014). The possible changes in plant
16 functioning during La Niña events are still not clarified. In particular, Malhi et al. (1999) reported
17 that for Amazon region in the South America El Niño periods are strongly associated with enhanced
18 dry seasons that probably result in increased carbon loss, either through water stress causing
19 reduced photosynthesis or increased tree mortality. Aiba and Kitayama (2002) examined the effects
20 of the 1997–98 El Niño drought on nine rainforests of Mount Kinabalu in Borneo using forest
21 inventory and showed that El Niño increased the tree mortality for lowland forests. However, it did
22 not affect the growth rate of the trees of upland forests (higher than 1,700 m) where mortality was
23 restricted by some understorey species only. Eddy covariance measurements of the CO₂ fluxes in a
24 tropical peat swamp forest in Central Kalimantan, Indonesia, for the period from 2002 to 2004,
25 provided by Hirano et al. (2007), showed that during the El Niño event in the period November-
26 December 2002 the annual net CO₂ release reached maximal values, mainly due to strong decrease
27 of GPP in the late dry season, because of dense smoke emitted from large-scale fires. Effects of El
28 Niño on annual RE in 2002 were insignificant.

29 There is a lack of experimental data on CO₂ and H₂O fluxes in mountainous rainforests in
30 equatorial regions of the Western Pacific, and on their response to ENSO. Hence, the main
31 objective of this study was to evaluate and quantify the impact of ENSO events on the main
32 components of CO₂ and H₂O fluxes in an old-growth mountainous tropical rainforest growing in
33 Central Sulawesi, Indonesia. The methodology used was analysis of long-term eddy covariance flux
34 measurement data.

35

1 **2. Materials and Methods**

2 **2.1 El Niño's types and intensity**

3 Nowadays, two types of ENSO can be distinguished: 1) the canonical or conventional El
4 Niño, which is characterised by SST anomalies located in the eastern Pacific near the South
5 American coast (Rasmusson and Carpenter, 1982) and 2) the Central Pacific El Niño or El Niño
6 Modoki (Larkin and Harrison, 2005; Ashok et al., 2007; Kug et al., 2009; Ashok and Yamagata,
7 2009; Gushchina and Dewitte, 2012). In 2003, a new definition of the conventional El Niño was
8 accepted by the National Oceanic and Atmospheric Administration (NOAA) of the USA, in
9 referring to the warming of the Pacific region between 5°N - 5°S and 170° - 120°W. According to
10 Ashok et al. (2007) the Central Pacific El Niño/El Niño Modoki - i.e. unusually high SST - occurs
11 roughly in the region between 160°E - 140°W and 10°N - 10°S.

12 As criteria to assess the intensity of ENSO events, a wide range of indexes based on
13 different combinations of sea level pressure and SST data in various areas of the Pacific are used.
14 For diagnostics of the central Pacific El Niño, the SST anomalies (in °C) in Nino4 region (5°N -
15 5°S and 160°E - 150°W) are broadly used (Figure 1). The monthly SST anomalies (in °C) in
16 Nino3.4 region (5°N - 5°S and 170° - 120°W) are used to diagnose both types of El Niño
17 phenomenon: canonical and Central Pacific (Download Climate Timeseries, 2013).

18

19 **2.2 Experimental site**

20 The tropical rainforest selected for the study is situated near the village Bariri in the southern
21 part of the Lore Lindu National Park of Central Sulawesi in Indonesia (1°39.47'S and 120°10.409'E
22 or UTM 51S 185482 m east and 9816523 m north) (Figure 1). The site is located on a large plateau
23 of several kilometres in size at about 1,430 m above sea level surrounded by mountain chains
24 surmounting the plane by another 300 m to 400 m. Within 500 m around the tower the elevation
25 varies between 1,390 and 1,430 metres. Wind field measurement with a sonic anemometer indicate
26 a slope of around 2-3°, which is similar to many Fluxnet sites. About 1,000 m to the east from the
27 experimental site, the forest is replaced by a meadow; in all other directions the forest extends
28 several kilometres (Ibrom et al., 2007).

29 According to the Köppen climate classification the study area relates to tropical rainforest
30 climate (*Af*) (Chen and Chen, 2013). Weather conditions of the region are mainly influenced by the
31 ITCZ. During the wet season (typically, from November to April) the area is influenced by very
32 moist northeast monsoons coming from the Pacific. Maximum precipitation during the observation
33 period from January 2004 to July 2008 was observed in April - with 258.0 ± 148.0 mm month⁻¹. The
34 drier season usually lasts from May to October. The precipitation minimum was observed in

1 September with 195.0 ± 48.0 mm month⁻¹. The September-October period was also characterised by
2 maximal incoming solar radiation, up to 650 ± 47.0 MJ m⁻² month⁻¹, mainly because of a significant
3 decrease of convective clouds, due to the reversing of oceanic northeast monsoon to a southeast
4 monsoon blowing from the Australian continent. The mean annual precipitation amount exceeded
5 2000 mm. The mean monthly air temperature varies between 19.4 °C and 19.7 °C. The mean annual
6 air temperature was 19.5 °C (Falk et al., 2005; Ibrom et al., 2007).

7 The vegetation at the experimental site is very diverse and representative for the
8 mountainous rainforest communities of Central Sulawesi. There are about 88 different tree species
9 per hectare. Among the dominant species are *Castanopsis accuminatissima* BL. (29%), *Canarium*
10 *vulgare* Leenh. (18%) and *Ficus spec.* (9.5%). The density of trees, with diameter at breast height
11 larger than 0.1 m, is 550 trees per ha. In addition, there is more than a 10-fold larger number of
12 smaller trees per hectare with stem diameter lower than 0.1 m. The total basal area of trees reached
13 53 m² per ha. Leaf area index (LAI) is about 7.2 m² m⁻². LAI has been estimated using an indirect
14 hemispherical photography approach with a correction for leaf clumping effects. The height of the
15 trees, with diameters at breast height larger than 0.1 m, varies between the lowest at 12 m and the
16 highest at 36 m. The mean tree height is 21 m (Ibrom et al., 2007).

17

18 **2.3 Flux measurements and gap filling**

19 CO₂ and H₂O fluxes were measured from 2004 to 2008 within the framework of the
20 STORMA project (Stability of Rainforest Margins in Indonesia, SFB 552), supported by the
21 German Research Foundation (DFG). Eddy covariance equipment for flux measurements was
22 installed on a meteorological tower of 70 m height at the 48 m level, i.e. ca. 12 m higher than the
23 maximal tree height. The measuring system consists of a three-dimensional sonic anemometer
24 (USA-1, Metek, Germany) and an open-path CO₂ and H₂O infrared gas analyzer (IRGA, LI-7500,
25 Li-Cor, USA) (Falk et al., 2005; Ibrom et al., 2007; Panferov et al., 2009). The open-path IRGA
26 was chosen due to its smaller power requirements compared to closed-path sensors. The sensor was
27 calibrated with calibration gases two times per year and showed no considerable sensitivity drift
28 within one year of operation. Turbulence data were sampled at 10 Hz and stored as raw data on an
29 industrial mini PC (Kontron, Germany). All instruments were powered by batteries, which were
30 charged by solar panels, mounted on the tower. The system is entirely self-sustaining and has been
31 proven to run unattended over a period of several months. Post-field data processing on eddy
32 covariance flux estimates was carried out strictly according to the established recommendations for
33 data analysis (Aubinet et al., 2012). In addition to the procedures described in Falk et al. (2005) and
34 Ibrom et al. (2007), we corrected the flux data for CO₂ or H₂O density fluctuations due to heat

1 conduction from the open-path sensor (Burba et al., 2008; Järvi et al., 2009) using finally the
2 suggested method as described in Reverter et al. (2011).

3 The system operated at ca. 70% of the time. Ca. 30% of the measured flux data were
4 negatively affected by rain and other unfavourable conditions and removed. From night time
5 ecosystem respiration data a friction velocity (u_*) threshold value of 0.25 m s^{-1} was estimated
6 (Aubinet et al., 2000), i.e. at u_* values above this threshold the measured night time flux became
7 independent from u_* . Night time flux values that were measured at $u_* < 0.25 \text{ m s}^{-1}$ were removed,
8 which left 15% of the measured night time flux data in the data set. For filling the gaps in the
9 measured Net Ecosystem Exchange (NEE) and evapotranspiration, net radiation, sensible and latent
10 heat flux records as well as to quantify GPP, RE and forest canopy transpiration the process-based
11 Mixfor-SVAT model (Olchev et al., 2002; 2008) was used.

12 Mixfor-SVAT is a one-dimensional model of the energy, H_2O and CO_2 exchange between
13 vertically structured mono- or multi-specific forest stands and the atmosphere. The main model
14 advantage is its ability both to describe seasonal and daily patterns of CO_2 and H_2O fluxes at
15 individual tree and entire ecosystem levels and to estimate the contributions of soil, different forest
16 layers, and various tree species into the total ecosystem fluxes taking into account individual
17 structure, biophysical properties and responses of plant species to changes in environmental
18 conditions. The model also allows to take into account the non-steady-state water transport in the
19 trees, rainfall interception, dew generation, turbulence and convection flows within the canopy and
20 plant canopy energy storage. As model input the measured meteorological variables (air
21 temperature, water vapor pressure, wind speed, precipitation, CO_2 concentration, global solar
22 radiation) are used. The model was tested with long-term meteorological and flux data from
23 different experimental sites including the investigated forest under well-developed turbulent
24 conditions and showed a good agreement over a broad spectrum of weather and soil moisture
25 conditions (Olchev et al., 2002; Falk et al., 2005; Falge et al., 2005; Olchev et al., 2008). Using the
26 model is superior to common statistical gap-filling approaches, because these depend on calibration
27 under all relevant weather conditions, including those that were systematically excluded when the
28 open-path sensor did not work, e.g. under rain. For this reason one might argue that statistical gap-
29 filling is biased by calibration during dry weather conditions. The process-based model is, however,
30 able to take these weather situations into account, because it is based on general physical principles.
31 As it was shown in previous studies the model is able to predict both CO_2 and water fluxes under
32 various weather and soil moisture conditions at sites where closed-path sensors were used (Olchev
33 et al., 1996; Falge et al., 2005).

34

2.4 Micrometeorological measurements

Air temperature, relative humidity and horizontal wind speed were measured at 4 levels above and at 2 levels inside the forest canopy using ventilated and sheltered thermo-hygrometers and cup anemometers (Friedrichs Co., Germany) installed on the tower. Short- and long-wave radiation components were measured below and above the canopy with CM6B and CG1 sensors (Kipp & Zonen, The Netherlands). Rainfall intensity was measured on top of the tower with a tipping bucket in a Hellman-type rain gauge. To fill the gaps in measuring records the meteorological data from an autonomic meteorological station, situated about 900 m away from the tower outside the forest on a nearby meadow, were used. For the analysis, the monthly mean values of air temperature and monthly sums of precipitation and solar energy were calculated.

2.5 Data analysis

To estimate the possible impact of ENSO events on CO₂ and H₂O fluxes in the tropical rainforest at Bariri the temporal variability of monthly NEE, GPP, RE and ET in periods with different ENSO intensity was analysed. To quantify the ENSO impacts on meteorological parameters and fluxes and to distinguish them from effects caused by the seasonal migration of the ITCZ, the intra-annual patterns of CO₂ and H₂O fluxes as well as meteorological conditions during the measuring period were also evaluated.

In the first step to assess the possible impact of ENSO events on meteorological parameters (global solar radiation (G), precipitation amount (P), air temperature (T) and CO₂ and H₂O fluxes), the correlation between the absolute values of monthly G, P, T, NEE, GPP, RE, ET and monthly SST-anomalies in Nino4 and Nino3.4 regions (Nino4 and Nino3.4 indexes) were analysed.

In the second step, we analyzed the correlation between the deviations of monthly meteorological parameter and flux values from their monthly averages over the entire measuring period and the Nino4/Nino3.4 indexes. The deviation in the case of GPP (ΔGPP) was estimated as

$$\Delta GPP_{Month, Year} = GPP_{Month, Year} - \frac{1}{N} \sum_{Year=2004}^{2008} GPP_{Month, Year}$$

where $GPP_{Month, Year}$ is total monthly GPP for a particular month (January to December) and corresponding year (2004 to 2008), $\frac{1}{N} \sum_{Year=2004}^{2008} GPP_{Month, Year}$ is monthly GPP for this particular month averaged for the entire measuring period (2004 to 2008); N is number of years. Positive values in ΔGPP , ΔRE , and ΔNEE indicate GPP, RE higher and NEE (carbon uptake) lower than average.

1 The typical timescale of full ENSO cycle is estimated be about 48-52 months (Setoh et al.,
2 1999) whereas the timescale of the main meteorological parameters (global solar radiation (G),
3 precipitation amount (P), air temperature (T)) is characterized by much higher month-to-month
4 variability even after annual trend filtering. In order to filter the high-frequency oscillation in the
5 time-series of atmospheric characteristics and monthly NEE, GPP, RE, ET anomalies the simple
6 centered moving average smoothing procedure was applied. The moving averages (MA) of
7 variables were calculated over 7 months (centered value ± 3 months).

8 Statistical analysis included both simple correlation and cross-correlation analysis
9 (Chatfield, 2004). Cross-correlation analysis was used to take into account the possible forward and
10 backward time shifts of maximal anomalies of meteorological parameters and CO₂ and H₂O fluxes
11 in respect to time of the ENSO culmination. To describe the relationships between atmospheric
12 fluxes and meteorological parameters the monthly non-smoothed values were used.

13

14 **3. Results**

15 During the measuring period, two El Niño (August 2004 - March 2005 and October 2006 -
16 January 2007) and one La Niña (November 2007 - April 2008) phenomena were observed. All
17 events had moderate intensity. Both warm events could be classified as the Central Pacific or
18 Modoki type, according to Ashok et al. (2007), since the SST-anomalies were centred in Nino3.4
19 and Nino4 regions (Figure 1).

20 Analysis of the intra-annual pattern of CO₂ and H₂O fluxes shows a relatively weak seasonal
21 variability (Figure 2). The maximal values of GPP were obtained during the second part of the drier
22 season - from August to October ($278 \pm 13 \text{ g C m}^{-2} \text{ month}^{-1}$) - which is also characterised by
23 maximal values of incoming solar radiation. The mean monthly air temperature in the period varied
24 from minimal values in August ($19.2 \pm 0.2 \text{ }^\circ\text{C}$) to maximal values in October ($19.8 \pm 0.2 \text{ }^\circ\text{C}$). The
25 minimal GPP values were obtained in transition periods between more wet and dry seasons - in
26 May - June and November - December (240 ± 15 and $249 \pm 21 \text{ g C m}^{-2} \text{ month}^{-1}$, respectively). These
27 periods are also characterised by minimal amounts of incoming solar radiation ($512 \pm 40 \text{ MJ m}^{-2}$
28 month^{-1}). Maximal RE ($206 \pm 10 \text{ g C m}^{-2} \text{ month}^{-1}$) and values were obtained in October, which
29 corresponds to the period of maximal air temperature and insolation. The local maximum of RE in
30 April - May ($199 \pm 4 \text{ g C m}^{-2} \text{ month}^{-1}$) is also well correlated with a small increase of the air
31 temperature in these months. The minimal RE was observed in February and June-August (174 ± 10
32 and $187 \pm 15 \text{ g C m}^{-2} \text{ month}^{-1}$, respectively). The intra-annual pattern of ET was closely related to the
33 seasonal variability of GPP. The maximum values of ET were also observed in October (136 ± 4
34 mm), in the month of maximal incoming solar radiation and highest values of air temperature. In

1 spite of a large amount of precipitation and a high air temperature during the period from March to
2 June, ET in this period was much lower than in September and October (e.g. 105 ± 8 mm in April).

3 Comparisons of monthly NEE, GPP, RE, ET and absolute values of SST-anomalies in
4 Nino4 and Nino3.4 regions (henceforth Nino4 and Nino3.4 indexes) indicate relatively low
5 correlations. Changes of the Nino4 index can explain about 12% of the observed variability in GPP
6 (coefficient of determination, $r^2=0.12$ under significance level $p<0.05$), 9% of RE ($r^2=0.09$, $p<0.05$),
7 9% of NEE ($r^2=0.09$, $p>0.05$), 6% of ET ($r^2=0.06$, $p<0.05$) and only about 1% of transpiration (TR)
8 ($r^2=0.01$, $p>0.05$). Similar values were obtained for the Nino3.4 index. In the periods of El Niño
9 peak phases (September 2004 - January 2005 and October 2006 - January 2007) the values ET and
10 GPP tend to increase in the study area. An increase of RE was indicated only during the second El
11 Niño event from October 2006 to January 2007. The effect of El Niño on NEE was insignificant.
12 The effect of La Niña on CO₂ and H₂O flux components was very small and manifested only in a
13 slight increase of NEE.

14 Analysis of the temporal variability of the centered moving average values of ΔGPP
15 (ΔGPP_{MA}) (Figure 3) in contrast to comparisons of absolute monthly GPP indicates a relatively high
16 correlation between ΔGPP_{MA} and both Nino4 ($r^2=0.52$, $p<0.05$) and Nino3.4 ($r^2=0.60$, $p<0.05$)
17 indexes. Close correlation between the intensity of ENSO events and ΔGPP_{MA} can be explained by
18 the influence of ENSO initiating processes and ENSO itself on total cloud amount in the region and,
19 as a result, on monthly sums of incoming G (Figure 4). Variability of G (ΔG_{MA}) is very closely
20 correlated with Nino4 and Nino3.4 indexes ($r^2=0.48$, $p<0.05$ for both indexes) (Figure 4) and it can
21 explain 69% of variability of GPP ($r^2=0.69$, $p<0.05$). The maximal deviations of ΔGPP_{MA} and
22 ΔG_{MA} from mean values (averaged for the entire measuring period) are occurring 2-3 months before
23 the peak phase of the ENSO events (Figure 5). The maximal cross-correlation coefficients in this
24 period reached 0.76 for ΔG_{MA} , and 0.86 - for ΔGPP_{MA} . The effect of T changes (ΔT) on ΔGPP is
25 very low ($r^2=0.01$, $p>0.05$).

26 The correlation between ΔT_{MA} and Nino4, Nino3.4 indexes are relatively low ($r^2=0.15$,
27 $p>0.05$ for Nino4 and $r^2=0.05$, $p>0.05$ for Nino3.4) and it can explain the very weak correlations
28 between ΔRE_{MA} and ENSO indexes ($r^2=0.10$, $p<0.05$ for Nino4 and $r^2=0.04$, $p>0.05$ for Nino3.4)
29 (Figures 3-4). The maximal deviations of T_{MA} and RE_{MA} from mean values (averaged for the entire
30 measuring period) are occurring 2 months after the peak phase of the ENSO events and it has
31 negative sign (Figure 5). The cross-correlation coefficient in this period is -0.53 ($p<0.05$).

32 Despite the relatively close dependence of ΔGPP_{MA} on ENSO intensity, the correlations
33 between ΔNEE_{MA} and Nino4, Nino3.4 indexes are lower ($r^2 = 0.31$, $p<0.05$ for Nino4 and $r^2 = 0.37$,
34 $p<0.05$ for Nino3.4), mainly because of their very low correlation during the first part of the
35 measuring period (before December 2005). During the second part of the considered period (from

1 June 2006 to June 2008) with one strong El Niño (October 2006 - January 2007) and one La Niña
2 (November 2004 - April 2008) events ΔNEE_{MA} and Nino4, Nino3.4 indexes are correlated much
3 better. It can be explained by the influence of ΔRE_{MA} on ΔNEE_{MA} dynamics that is mainly
4 governed by temperature variability and which is, as already mentioned, very poorly correlated with
5 Nino4/Nino3.4 indexes (Figures 3-4).

6 Taking into account that the monthly anomalies of NEE might be biased by a still
7 unaccounted advection effects at night-time, despite u^* filtering, we additionally examined NEE at
8 midday (10:00-14:00), when turbulent mixing is typically well developed. Data analysis based on
9 midday NEE shows a similar clear relationship with the ENSO index (Figure 6) with $r^2 = 0.59$
10 under $p < 0.05$. The maximal deviations of both NEE_{MA} and midday NEE_{MA} from the their mean
11 values occurred simultaneously within the peak phase of the ENSO events (Figure 5).

12 Analysis of the temporal variability of the moving average values of monthly ET (ΔET_{MA})
13 showed a high correlation to ENSO activity as well: $r^2 = 0.72$, $p < 0.05$ for Nino4 and $r^2 = 0.70$,
14 $p < 0.05$ for Nino3.4 (Figure 7), probably also triggered by G_{MA} , which in turn correlated strongly
15 with both the Nino4 and the Nino3.4 index. Periods of extreme ΔET_{MA} values and maximal ENSO
16 intensity occurred simultaneously (Figure 5). Correlations between ΔET and ΔT , as well as between
17 ΔET and ΔP , are insignificant - $r^2 = 0.09$ ($p > 0.05$) and $r^2 = 0.01$ ($p > 0.05$), respectively. However,
18 figures 4 and 5 clearly show a time delay in ΔP_{MA} oscillation, relative to Nino4 and Nino3.4
19 patterns. The maximal negative deviations of ΔP_{MA} are observed about eight months before (cross-
20 correlation between ΔP_{MA} and Nino 4 index 0.72, $p < 0.05$) and maximal positive deviation of ΔP_{MA}
21 - about four-five months after the peak phases of ENSO (cross-correlation between ΔP_{MA} and Nino
22 4 index - 0.40, $p < 0.05$), respectively.

23 To explain a very low sensitivity of ET to P changes, we analysed the intra-annual
24 variability of the ratio between ET and potential evaporation (PET), as well as between ET and P.
25 PET was derived using the well-known Priestley and Taylor (1972) approach and it is equal to
26 evaporation from wet ground or open water surface.

27 The mean annual ET during the measuring period is considerably lower than P
28 ($ET/P = 0.742$). Over the annual course, the ratio varied between 0.58 (in March and November) to
29 1.85 (in August and October). During dry periods before the positive phase of ENSO, the mean
30 values of the ET/P ratio grow up to 1.9-2.1. During the periods of negative Nino4 and Nino3.4
31 anomalies the mean monthly ET/P ratio fell, in some months, down to 0.3. Correlation analysis of
32 temporal variability of $\Delta(ET/P)$ and $\Delta(ET/P)_{MA}$ ratios and Nino4 and Nino3.4 indexes (Figure 7) did
33 not show any statistically significant relationships. However, it should be mentioned that the
34 temporal pattern of $\Delta(ET/P)$ and $\Delta(ET/P)_{MA}$ is characterised by two peaks that were observed in
35 July of 2005 and April 2007, about 6-8 months prior to the El Niño culmination (Figure 7).

1 The monthly mean ET/PET ratio has a feeble intra-annual course with maximum in June
2 (0.93±0.03) and with minima in February and October (0.84±0.06). The averaged annual ET/PET
3 ratio for the entire measuring period was 0.880±0.055. The minimal values of (ET/PET)_{MA}
4 ((ET/PET)_{MA}=0.81) were observed during the El Niño culmination in 2005-2006, and the maximal
5 values, during the period of maximal intensity of La Niña in 2008 ((ET/PET)_{MA}=0.93). Thus,
6 monthly ET rates are relatively close to PET values during the whole year including the periods of
7 maximal ENSO activity. The relative soil water content of the upper 30 cm horizon calculated using
8 the Mixfor-SVAT model during the entire period of the field measurements, including the periods
9 with maximal values of the ET/P ratio, was always higher than 80%. This, together with the
10 ET/PET ratio, is a clear indicator of permanently sufficient soil moisture conditions in the study
11 area, including periods of El Niño and La Niña culminations, explaining the very low sensitivity of
12 ΔET to ΔP .

13

14 **4. Discussion**

15 **4.1. Uncertainty of the analysis**

16 Eddy covariance flux measurements in tropical mountainous conditions are challenging. Our
17 tower and eddy covariance system was designed to minimise power consumption by using an open-
18 path sensor, which had the consequence that rainy conditions systematically caused gaps in the flux
19 data. To minimise a potential bias on the flux sums, we used a process-based forest model that is
20 not biased by a lack of data in wet conditions as the often used statistical gap-filling algorithms
21 (Reichstein et al., 2005, see also section 2.3). The weather in the tropics typically has a relatively
22 high percentage of calm nights. The selected forest is located on a plateau in a mountainous region
23 and this increases the risk of CO₂ rich air draining downhill in calm night. We investigated this
24 effect very carefully and found that the CO₂ fluxes showed a very clear u_* threshold above which
25 the night time CO₂ emission rates did not depend on u_* anymore. Using only data from nights with
26 sufficient turbulence ($u_* > u_*$ threshold value) we minimised advection and drainage affecting the
27 NEE estimates. Also, here we benefitted from the use of the process-based model for gap-filling.
28 We then analysed the statistical relationships between our gap-filled monthly fluxes with climate
29 anomaly indices and corroborated these analyses also with midday NEE data only. As time data are
30 independent from night time data, we made sure that our analysis was not affected by night time
31 flux loss. The correlations with midday data and ENSO indices were very similar to those with
32 daily mean NEE data. This demonstrated the robustness of our analysis.

33 In addition we compared the the model predicted mean annual soil respiration rate with soil
34 CO₂ efflux data that were measured in the study region with soil chambers (van Straaten et al.,

1 2011). The Mixfor-SVAT model estimated an average annual soil respiration rate of $1110 \pm 30 \text{ g C}$
2 $\text{m}^{-2} \text{ yr}^{-1}$ for the investigated site. This value was very close to the measured average soil CO_2 efflux
3 of for the central Sulawesi region of $1170 \text{ g C m}^{-2} \text{ yr}^{-1}$ which shows realistic behavior of the model.

4 The relatively high annual NEE sums need further investigation. After applying all
5 corrections including the correction for open-path sensor heating, and after gap filling we found an
6 average annual uptake of $729 \pm 32 \text{ g C m}^{-2} \text{ yr}^{-1}$ (standard deviation between 5 different years). This
7 value is higher as the range found in lowland rain forests, i.e. ranging from e.g. 75 to 538 g C m^{-2}
8 yr^{-1} (Luyssaert et al., 2007). The clarification of this very interesting phenomenon, maybe relating
9 to the site history and regrowth after selected use of large individual trees by the local population,
10 lies however not within the scope of this article.

11

12 **4.2 Effects of large scale climate anomalies on carbon and water exchange in the** 13 **investigated site**

14 The main components of carbon and water balances in the tropical rainforest showed a high
15 correlation between Nino4 and Nino3.4 SST anomalies and $\Delta\text{GPP}_{\text{MA}}$ and $\Delta\text{ET}_{\text{MA}}$ values over the
16 entire measuring period. The smoothing procedure allowed us to remove the high-frequency month-
17 to-month oscillations in the time-series of atmospheric characteristics. These are caused by local
18 and regional circulation processes that are not directly connected with ENSO activity and disturb
19 thus the analysis. The relationships between $\Delta\text{GPP}_{\text{MA}}$, $\Delta\text{ET}_{\text{MA}}$ and Nino4 and Nino3.4 indexes are
20 governed via the dependency of the incoming solar radiation on ENSO development – surface water
21 warming in Nino 3.4 and 4 regions generally results in a decrease of cloudiness above the study
22 region and thus in an increase of incoming solar radiation. The high correlation of monthly GPP and
23 ET rates with incoming and absorbed solar radiation at this site is well described (e.g. Ibrom et al.,
24 2008). The effects of monthly air temperature and precipitation changes on ΔGPP and ΔET
25 variability are on the contrary relatively poor. $\Delta\text{T}_{\text{MA}}$, $\Delta\text{P}_{\text{MA}}$ and ENSO intensity are not very much
26 related.

27 The cross-correlation analysis (Fig. 5) shows that the $\Delta\text{GPP}_{\text{MA}}$ and $\Delta\text{G}_{\text{MA}}$ have a small 2-3
28 month backward shift relatively to the course of Nino4 SST, i.e. the maxima in GPP_{MA} occur earlier
29 than ENSO culmination in the central Pacific (Nino4 SST anomaly). The maximal values of $\Delta\text{E}_{\text{MA}}$
30 occurred simultaneously with El Niño and La Niña culminations. Such an effect of El Niño
31 episodes on G can be explained, as mentioned above, by a decrease of the cloud cover in the region
32 of Indonesia, due to the El Niño-associated shift of the Walker circulation cell, and corresponding
33 zone of deep convection, from the maritime continent of Indonesia toward the dateline following
34 SST anomalies displacement. El Nino usually begins in April, and toward August-September the
35 ascending branch of the Walker cell leaves Indonesia and migrates eastward to the Pacific.

1 Therefore, 3-4 months before the El Niño culmination in December-January, a decrease in cloud
2 amount is observed over Indonesia. Weakening of El Niño, in turn, leads to a backward shift of
3 intensive convection zone westward. It can result in increasing precipitation amounts in the region
4 during the second half of the wet period after passing the maximal El Niño activity and also the
5 gradual increase of the cloudiness and decrease of incoming solar radiation. The opposite effect
6 takes place during the La Niña with similar phase shift: simultaneously, with the spreading of a
7 negative SST anomaly over the Pacific, the increasing of deep convection over Indonesia occurs,
8 which results in an increase of cloudiness and precipitation, being more pronounced as it falls into
9 the dry period of the year. The lower panels of Figure 4 indicate however, that the decrease of
10 radiation due to increase of cloudiness does not depend linearly on La Nina intensity, reaching a
11 saturation state at approximately $-20..-30 \text{ MJ m}^{-2} \text{ month}^{-1}$.

12 A relatively poor correlation between ΔT_{MA} patterns and ENSO activity and an insignificant
13 influence of ΔT on ΔGPP and ΔET can be mainly explained by the small intra-annual amplitude of
14 the air temperature in the study area not exceeding $1.0 \text{ }^\circ\text{C}$, as well as by the low dependence of the
15 air temperature on incoming solar radiation. The mean monthly temperatures ranged in the intra-
16 annual course between $19.5 \text{ }^\circ\text{C}$ and $20.5 \text{ }^\circ\text{C}$. Maximal air temperatures do not exceed $28.5 \text{ }^\circ\text{C}$, even
17 on sunny days. Such optimal thermal conditions with high precipitation amount provide sufficient
18 soil moistening and relatively comfortable conditions for tree growth during the whole year. As is
19 was already mentioned even during the El Niño culmination in 2005-2006 the ET/PET did not
20 decrease below 0.74, $(\text{ET}/\text{PET})_{\text{MA}} > 0.81$, and the relative soil water content of the upper 30 cm
21 horizon was always higher than 80%.

22 The analysis of absolute and relative changes of GPP and ET during the periods of maximal
23 El Niño and La Niña activities showed that GPP during the El Niño culminations of 2005 and 2007
24 increased by about $20 \text{ g C m}^{-2} \text{ month}^{-1}$ (6-7%). $\Delta \text{GPP}_{\text{MA}}$ was about $9 \text{ g C m}^{-2} \text{ month}^{-1}$ (2-3%), ΔET
25 - about 40 mm month^{-1} (about 30%) and $\Delta \text{ET}_{\text{MA}}$ - about 10 mm month^{-1} (6-7%). Thus, the maximal
26 ΔGPP was two times lower than the mean annual amplitude of GPP (Figure 2). The maximal ΔET
27 was equal to the annual amplitude of ET (Figure 2). During the La Niña culmination of 2008 the
28 maximal relative changes of GPP were higher than the relative changes observed during El Niño
29 events: ΔGPP was about $-22 \text{ g C m}^{-2} \text{ month}^{-1}$ (8%), $\Delta \text{GPP}_{\text{MA}}$ - about $-12 \text{ g C m}^{-2} \text{ month}^{-1}$ (4%). The
30 maximal decrease of ΔET in the period was relatively small: ΔET - about $-12 \text{ mm month}^{-1}$ (10%)
31 and $\Delta \text{ET}_{\text{MA}}$ - about -5 mm month^{-1} (4%). ΔET was about 3 times lower than the mean annual
32 amplitude of ET. Interestingly the radiation dependent GPP (as represented by smoothed 7 month
33 mean) does not demonstrate any prolonged constant period during La Nina phases though the
34 radiation does. During the first cold event the GPP-reduction is not as strong as during the second
35 one, although the G-reductions are nearly of same strength. It could be assumed that in the first case

1 the effect of radiation decrease on GPP was compensated by other factors like slight increase of the
2 air temperature.

3 Additionally, we investigated the influence of other climatic anomalies in the region on CO₂
4 and H₂O fluxes of the tropical rainforest, such as the Madden–Julian oscillation (MJO) and the
5 Indian Ocean Dipole (IOD). The MJO is characterised by an eastward propagation of large regions
6 of enhanced and suppressed deep convection from the Indian ocean toward central Pacific (Zhang,
7 2005). Each MJO cycle lasts approximately 30–60 days and includes wetter (positive) and drier
8 (negative) phases. As an estimation of deep convection intensity in the tropics, the outgoing long-
9 wave radiation (OLR) measured at the top of the atmosphere is commonly used. It was recently
10 shown that 6-12 months prior to the onset of an El Niño episode a drastic intensification of the MJO
11 occurs in the Western Pacific (Zhang and Gottschalck, 2002; Lau, 2005; Hendon et al., 2007;
12 Gushchina and Dewitte, 2011). Furthermore, MJO behaviour varies significantly during the ENSO
13 cycle: it is significantly decreased during the maxima of conventional El Niño episodes, while it is
14 still active during the peak phase of central Pacific events. MJO rarely occurs during La Niña
15 episodes (Gushchina and Dewitte, 2012). As MJO is strongly responsible for intra-seasonal
16 variation of precipitation in the study region, the occurrence of MJO events was compared to the
17 significant anomalies of ET/P ratio and of key meteorological variables. No evidence of MJO
18 influence is observed: the positive and negative anomalies of ET/P ratio are associated to positive,
19 negative and zero anomalies of OLR, filtered in the MJO interval. Also, no significant relation
20 emerged from the correlation analysis.

21 Correlations between MJO index (Wheeler and Kiladis, 1999; Gushchina and Dewitte,
22 2011), and the deviations of key meteorological parameters from monthly averages during the study
23 period were very low: $r^2 = 0.03$ for T, $r^2 = 0.03$ for P and $r^2 = 0.01$ for G ($p > 0.05$, in all cases).

24 The Indian Ocean Dipole (IOD) is characterised by changes of the SST in the western
25 Indian Ocean, resulting in intensive rainfall in the western part of Indonesia during the positive
26 phase and corresponding precipitation reduction during the negative phase (Saji et al., 1999). To
27 find a possible influence of IOD events on temporal variability of meteorological parameters and
28 CO₂ and H₂O fluxes, the monthly mean IOD index (Dipole Mode Index, DMI) was used. Results
29 showed that with respect to the western part of Indonesia situated close to Indian Ocean the IOD
30 phenomenon has no significant impact on meteorological conditions and fluxes of the area of
31 Central Sulawesi.

32 Our case study showed a high sensitivity of the main components of CO₂ and H₂O fluxes of
33 the investigated mountainous tropical rainforest in Bariri to El Niño and La Niña phenomena as
34 well as a low sensitivity to IOD and MJO events. The time lag between the respective indices and
35 their effect on the fluxes at our site indicates that the timing and the extent of the effects are site

1 specific. The fluxes respond to the local weather and only indirectly to the large scale weather
2 anomalies, i.e. in the way the local weather is affected by the large scale weather phenomena. The
3 observed phenomena are thus not representative for all mountainous forest sites in the tropics. The
4 conclusion is that large scale weather anomalies do have systematic effects on local fluxes but the
5 timing and the extent are likely to differ across different regions.

6 Even though remote sensing analyses have shown that the site is representative for the
7 region (Ibrom et al., 2007; Popastin et al., 2012), the response to ENSO might differ in the region
8 due to differences in altitude and land-use (Erasmi et al. 2009). In general, anthropogenic
9 deforestation has removed most parts of lowland forests so that the remaining forest cover consists
10 mostly of mountainous forests. At the moment, there are no other FLUXNET sites situated in
11 equatorial mountainous rainforests of South-East Asia with which we could directly compare our
12 findings and investigate whether similar response to ENSO can be observed. Most of the existing
13 FLUXNET sites (AsiaFlux) are not comparable with the investigated site as they are situated in
14 subequatorial and tropical climate zones. These are characterized by higher seasonality of air
15 temperature and precipitation compared to our equatorial site. Thus, our site provides a unique
16 opportunity to investigate the response of an equatorial mountainous rainforest to ENSO in the
17 Western Pacific region.

18

19 **5. Conclusions**

20 CO₂ and H₂O fluxes in the mountainous tropical rainforest in Central Sulawesi in Indonesia
21 showed a high sensitivity of monthly GPP and ET to ENSO intensity for the period from January
22 2004 to June 2008. This was mainly governed by the high dependency of incoming solar radiation
23 (G) to Niño4 and Niño3.4 SST changes and the strong sensitivity of GPP and ET on G .

24 Interestingly, we observed time shifts between the SST anomalies and smoothed GPP
25 anomalies driven by radiation anomalies. The maximal deviations of GPP and G from their mean
26 values occurred 2-3 months before the peak phase of the ENSO events. The effect of ENSO
27 intensity on ecosystem respiration, RE, was relatively low, mainly due to its weak effect on air
28 temperature. Anyway, the small cross-correlation between RE and ENSO intensity had a
29 compensatory effect on the respective timing of NEE, which thus was - like evapotranspiration - in
30 synchrony with El Niño culminations. Unlike the observations in other tropical sites, precipitation
31 variations had no influence on the CO₂ and H₂O fluxes at study site, mainly due to the permanently
32 sufficient soil moisture condition in the study area.

1 Other climatic anomalies in the Western Pacific region, such as the Indian Ocean Dipole and
2 the Madden–Julian oscillation, did not show any significant effect on neither the meteorological
3 conditions nor the CO₂ and H₂O fluxes in the investigated rainforest in Central Sulawesi.

4 It is important to emphasise that the observation period does not cover any period with
5 extreme El Niño events, such as, e.g., the 1982-83 and 1997-98 events, when the anomaly of
6 Niño3.4 SST, during several months, exceeded 2.6°C and more significant changes of surface water
7 availability were observed. Also, in lowland parts of Sulawesi, characterised by higher temperatures
8 and lower precipitation, the vegetation response to ENSO events is likely to be different and more
9 pronounced (Erasmí et al., 2009).

10 All observed ENSO events during the selected period are classified as Central Pacific type.
11 Recently, Yeh et al. (2009) showed that under projected climate change the proportion of Central
12 Pacific ENSO events might increase. Furthermore, Cai et al. (2014, 2015) showed that current
13 projections of climate change for the 21st century suggest an increased future likelihood of both El
14 Niño and La Niña events. Based on the results of our study, potential increases in ENSO activity
15 would result in an increased variability of the CO₂ and H₂O exchange between atmosphere and the
16 tropical rainforests in these and similar regions.

18 **Acknowledgement**

19 The study was supported by the German Research Foundation under the projects "Stability
20 of Rainforest Margins in Indonesia", STORMA (SFB 552), "Ecological and Socioeconomic
21 Functions of Tropical Lowland Rainforest Transformation Systems (Sumatra, Indonesia)" (SFB
22 990) and KN 582/8-1. The Russian Science Foundation (grant RSCF 14-27-00065) supports A.
23 Olchev in part of the model development.

25 **Reference**

- 26 1. Aiba, S., and Kitayama, K.: Effects of the 1997-98 El Niño drought on rain forests of Mount
27 Kinabalu, Borneo, *Journal of Tropical Ecology*, 18, 215–230, 2002
- 28 2. Ashok, K., Behera, S. K., Rao S. A., Weng H., Yamagata, T.: El Niño Modoki and its possible
29 teleconnection. *J. Geophys. Res.* 112, C11007, doi:10.1029/2006JC003798, 2007
- 30 3. Ashok, K. and Yamagata, T.: The El Niño with a difference. *Nature*, 461, 481-484, 2009
- 31 4. Aubinet, M., A. Grelle, A. Ibrom, U. Rannik, J. Moncrieff, T. Foken, A. S. Kowalski, P. H.
32 Martin, P. Berbigier, C. Bernhofer, R. Clement, J. Elbers, A. Granier, T. Grunwald, K.
33 Morgenstern, K. Pilegaard, C. Rebmann, W. Snijders, Valentini R. and Vesala T.: Estimates of

- 1 the annual net carbon and water exchange of forests: The EUROFLUX methodology.
2 *Advances In Ecological Research*, 30, 113-175, 2000
- 3 5. Aubinet, M., Vesala, T., and Papale, D. (Eds.): *Eddy Covariance: A Practical Guide to*
4 *Measurement and Data Analysis*. Springer Atmospheric Sciences, Springer Verlag, Dordrecht,
5 The Netherlands, 438 pp., 2012
- 6 6. Burba, G.G., McDermitt, D.K., Grelle, A., Anderson, D.J., Xu, L.: Addressing the influence of
7 instrument surface heat exchange on the measurements of CO₂ flux from open-path gas
8 analyzers. *Global Change Biology*, 14, 1-23, 2012
- 9 7. Cai, W., Borlace, S., Lengaigne, M., van Rensch, P., Collins, M., Vecchi, G., Timmermann, A.,
10 Santoso, A., McPhaden, M.J., Wu, L., England, M.H., Wang, G., Guilyardi, E. and Jin, F.-F.:
11 Increasing frequency of extreme El Niño events due to greenhouse warming. *Nature Climate*
12 *Change*, 4, 111-116, 2014
- 13 8. Cai, W., Wang, G., Santoso, A., McPhaden, M., Wu, L., Jin, F-F., Timmermann, A., Collins,
14 M., Vecchi, G., Lengaigne, M., England, M., Dommenges, D., Takahashi, K., Guilyardi, E.:
15 More frequent extreme La Niña events under greenhouse warming. *Nature Climate Change*, 5,
16 132-137, 2015
- 17 9. Chatfield, C.: *The Analysis of Time series, An Introduction*, sixth edition. Chapman &
18 Hall/CRC, New York, 333 pp., 2004
- 19 10. Chen, D. and Chen, H. W.: Using the Koppen classification to quantify climate variation and
20 change: An example for 1901-2010. *Environmental Development*, 6, 69-79, 2013
- 21 11. Ciais, P., Piao, S.L., Cadule, P., Friedlingstein, P., and Chedin, A.: Variability and recent trends
22 in the African terrestrial carbon balance. *Biogeosciences*, 6, 1935-1948, 2009
- 23 12. Clark, D.A., and Clark, D.B.: Climate-induced variation in canopy tree growth in a Costa Rican
24 tropical rain forest. *Journal of Ecology*, 82, 865-872, 1994
- 25 13. Download Climate Timeseries: http://www.esrl.noaa.gov/psd/gcos_wgsp/Timeseries/, 24 April
26 2013
- 27 14. Erasmi, S., Propastin, P., Kappas, M., and Panferov, O.: Patterns of NDVI variation over
28 Indonesia and its relationship to ENSO during the period 1982-2003, *J Climate*, 22(24), 6612–
29 6623, 2009
- 30 15. Falge, E., Reth, S., Brüggemann, N., Butterbach-Bahl, K., Goldberg, V., Oltchev, A., Schaaf,
31 S., Spindler, G., Stiller, B., Queck, R., Köstner, B., Bernhofer, C.: Comparison of surface
32 energy exchange models with eddy flux data in forest and grassland ecosystems of Germany. *J.*
33 *Ecological Modelling*, 188 (2-4), 174-216, 2005

- 1 16. Falk U., Ibrom A., Kreilein H., Oltchev A., and Gravenhorst, G.: Energy and water fluxes
2 above a cacao agroforestry system in Central Sulawesi, Indonesia, indicate effects of land-use
3 change on local climate *Met. Zeitsch.*, 14(2), 219-225, 2005
- 4 17. FAO: Global forest resources assessment 2010: Main report, FAO Forestry Paper 163, Rome,
5 Italy, 340 pp., 2010
- 6 18. Feely, R.A., Wanninkhof, R., Takahashi, T., and Tans, P.: Influence of El Niño on the
7 equatorial Pacific contribution to atmospheric CO₂ accumulation. *Nature* 398, 597-601, 1999
- 8 19. Fisher, J.B., Sikka, M., Sitch, S., Ciais, P., Poulter, B., Galbraith, D., Lee, J.-E., Huntingford,
9 C., Viovy, N., Zeng, N., Ahlstrom, A., Lomas, M.R., Levy, P.E., Frankenberg, C., Saatchi, S.,
10 and Malhi, Y.: African tropical rainforest net carbon dioxide fluxes in the twentieth century.
11 *Phil Trans R Soc B*, 368, 20120376, <http://dx.doi.org/10.1098/rstb.2012.0376>, 2013
- 12 20. Gerold, G., Leemhuis, C.: Effects of “ENSO-events” and rainforest conversion on river
13 discharge in Central Sulawesi (Indonesia). In: *Tropical Rainforests and Agroforests under*
14 *Global Change Environmental Science and Engineering*, T. Tschardt, Ch. Leuschner, E.
15 Veldkamp, H. Faust, E. Guhardja, A. Bidin (Eds), 327-350, 2010
- 16 21. Grace, J., Lloyd, J., McIntyre, J., Miranda, A., Meir, P., Miranda, H., Nobre, C., Moncrieff,
17 J.B., Massheder, J.M., Malhi, Y., Wright, I., and Gash, J.C.: Carbon dioxide uptake by an
18 undisturbed tropical rain forest in south-west Amazonia, 1992 to 1993. *Science*, 270, 778-780,
19 1995
- 20 22. Grace, J., Malhi, Y., Lloyd, J., McIntyre, J., Miranda, A.C., Meir, P., and Miranda, H.S.: The
21 use of eddy covariance to infer the net carbon uptake of Brazilian rain forest. *Global Change*
22 *Biology*, 2, 209-218, 1996
- 23 23. Graf, H.-F., and Zanchettin, D.: Central Pacific El Niño, the “subtropical bridge,” and Eurasian
24 climate, *J. Geophys. Res.*, 117, D01102, doi:10.1029/2011JD016493, 2012
- 25 24. Gushchina, D., and Dewitte, B.: The relationship between intraseasonal tropical variability and
26 ENSO and its modulation at seasonal to decadal timescales, *Cent. Eur. J. Geosci.*, 1(2), 175-
27 196, 2011, DOI: 10.2478/s13533-011-0017-3
- 28 25. Gushchina, D., and Dewitte, B.: Intraseasonal tropical atmospheric variability associated to the
29 two flavors of El Niño. *Month. Wea. Rev.*, 140, (11). 3669-3681, 2012
- 30 26. Hansen, M.C., Potapov, P. V., Moore, R., Hancher, M., Turubanova, S.A., Tyukavina, A.,
31 Thau, D., Stehman, S.V., Goetz, S.J., Loveland, T.R., Komardecky, A. Egorov, A., Chini, L.,
32 Justice, C.O., and Townshend, J.R.G.. High-Resolution Global Maps of 21st-Century Forest
33 Cover Change. *Science*, 342, 850-853, 2013

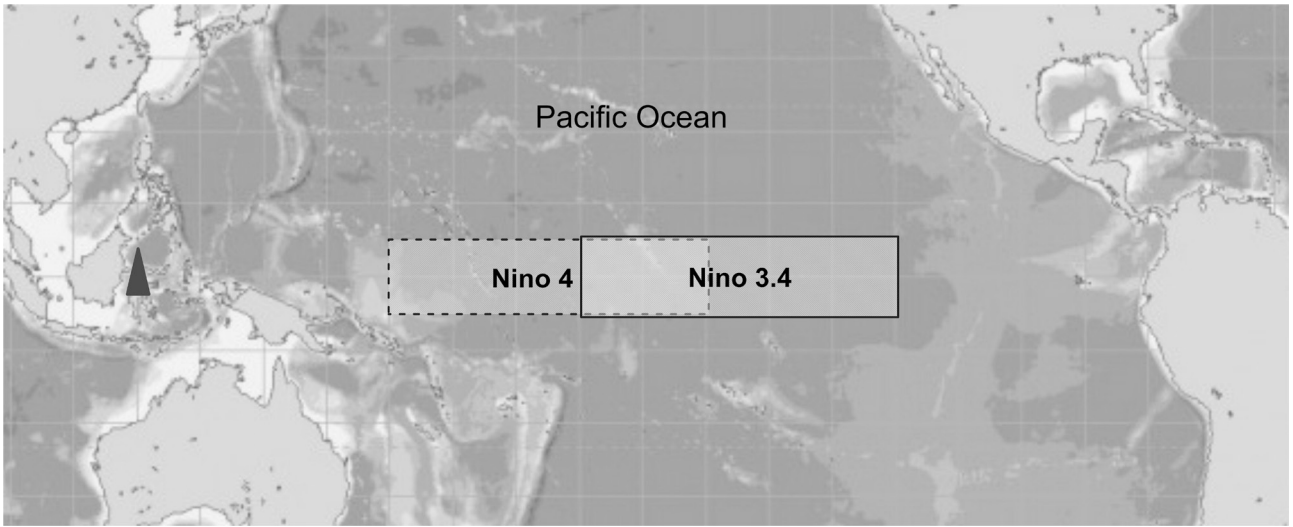
- 1 27. Hirano, T., Segah, H., Harada, T., Limin, S., June, T., Hirata, R., and Osaki, M.: Carbon
2 dioxide balance of a tropical peat swamp forest in Kalimantan, Indonesia. *Global Change*
3 *Biology*, 13, 412–425. doi: 10.1111/j.1365-2486.2006.01301.x, 2007
- 4 28. Ibrom, A., Olchev, A., June, T., Ross, T., Kreilein, H., Falk, U., Merklein, J., Twele, A.,
5 Rakkibu, G., Grote, S., Rauf, A., and Gravenhorst, G.: Effects of land-use change on matter and
6 energy exchange between ecosystems in the rain forest margin and the atmosphere. In *The*
7 *stability of tropical rainforest margins: Linking ecological, economic and social constraints*.
8 Eds. T. Tschardtke, C. Leuschner, M. Zeller, E. Guhardja and A. Bidin, Springer Verlag,
9 Berlin, pp. 463 – 492, 2007
- 10 29. Ibrom, A., Oltchev, A., June, T., Kreilein, H., Rakkibu, G., Ross, Th., Panferov, O.,
11 Gravenhorst, G.: Variation in photosynthetic light-use efficiency in a mountainous tropical rain
12 forest in Indonesia. *Tree Physiology*, 28(4), 499–508, 2008
- 13 30. Järvi, L., Mammarella, I., Eugster, W., Ibrom, A., Siivola, E., Dellwik, E., Keronen, P., Burba,
14 G., Vesala, T.: Comparison of net CO₂ fluxes measured with open- and closed-path infrared gas
15 analyzers in urban complex environment. *Boreal Environmental Research*, 14, 499–514, 2009
- 16 31. Kug, J.-S., Jin, F.-F., and An, S.-I.: Two types of El Niño events: Cold tongue El Niño and
17 warm pool El Niño, *J. Climate*, 22, 1499–1515, 2009
- 18 32. Larkin, N. K., and Harrison, D.E.: Global seasonal temperature and precipitation anomalies
19 during El Niño autumn and winter. *Geophysical Research Letters*, 32, L13705, 2005,
20 doi:10.1029/2005GL022738.
- 21 33. Lau, W. K. M.: El Niño Southern Oscillation connection. *Intraseasonal Variability of the*
22 *Atmosphere-Ocean Climate System*, W. K. M. Lau, and D. E. Waliser., Eds., Praxis
23 Publishing, Chichester, UK, 271-300, 2005
- 24 34. Lewis, S.L., Lopez-Gonzalez, G., Sonke, B., Affum-Baffoe, K., Baker, T.R., Ojo, L.O.,
25 Phillips, O.L., Reitsma, J.M., White, L., Comiskey, J.A., Djuikouo, K. M.-N., Ewango, C.E.N.,
26 Feldpausch, T.R., Hamilton, A.C., Gloor, M., Hart, T., Hladik, A., Lloyd, J., Lovett, J.C.,
27 Makana, J.-R., Malhi, Y., Mbago, F.M., Ndangalasi, H.J., Peacock, J., Peh, K. S.-H., Sheil, D.,
28 Sunderland, T., Swaine, M.D., Taplin, J., Taylor, D., Thomas, S.C., Votere, R. and Woll, H.:
29 Increasing carbon storage in intact African tropical forests. *Nature*, 457: 1003-1006, 2009
- 30 35. Luysaert, S., Inglima, I., Jung, M., Richardson, A.D., Reichstein, M., Papale, D., Piao, S.L.,
31 Schulze, E.-D., Wingate, L., Matteucci, G., Aragao, L., Aubinet, M., Beer, C., Bernhofer, C.,
32 Black, K.G., Bonal, D., Bonnefond, J.-M., Chambers, J., Ciais, P., Cook, B., Davis, K.J.,
33 Dolman, A.J., Gielen, B., Goulden, M., Grace, J., Granier, A., Grelle, A., Griffis, T. Grünwald,
34 T., Guidolotti, G., Hanson, P.J., Harding, R., Hollinger, D.Y., Hutyrá, L.R., Kolari, P. Kruijt,
35 B., Kutsch, W., Lagergren, F., Laurila, T., Law, B.E., Le Maire, G., Lindroth, A., Loustau, D.,

- 1 Malhi, Y., Mateus, J., Migliavacca, M., Misson, L., Montagnani, L., Moncrieff, J., Moors, E.,
2 Munger, J.W., Nikinmaa, E., Ollinger, S.V., Pita, G., Rebmann, C., Roupsard, O., Saigusa, N.,
3 Sanz, M.J., Seufert, G., Sierra C., Smith, M.-L., Tang, J., Valentini, R., Vesala T. and Janssens,
4 I.A.: CO₂ balance of boreal, temperate, and tropical forests derived from a global database.
5 *Global Change Biology* 13(12), 2509-2537, 2007
- 6 36. Malhi, Y., Baldocchi, D.D., and Jarvis, P.G.: The carbon balance of tropical, temperate and
7 boreal forests. *Plant Cell and Environment*, 22, 715-740, 1999
- 8 37. Malhi, Y.: The carbon balance of tropical forest regions, 1990–2005, *Current Opinion in*
9 *Environmental Sustainability*, 2(4), 237–244, 2010
- 10 38. Moser, G., Schuldt, B., Hertel, D., Horna, V., Coners, H., Barus, H., and Leuschner, C.:
11 Replicated throughfall exclusion experiment in an Indonesian perhumid rainforest: wood
12 production, litter fall and fine root growth under simulated drought. *Global Change Biology*,
13 20, 1481–1497, doi: 10.1111/gcb.12424, 2014
- 14 39. Oltchev, A., Constantin, J., Gravenhorst, G., Ibrom, A., Heimann, J., Schmidt, J., Falk, M.,
15 Morgenstern, K., Richter, I. and Vygodskaya, N. Application of a six-layer SVAT model for
16 simulation of evapotranspiration and water uptake in a spruce forest. *Physics and Chemistry of*
17 *the Earth*, 21(3), 195-199, 1996
- 18 40. Oltchev, A., Cermak, J., Nadezhdina, N., Tatarinov, F., Tishenko, A., Ibrom, A., Gravenhorst,
19 G.: Transpiration of a mixed forest stand: field measurements and simulation using SVAT
20 models. *J. Boreal Environmental Reserach*, 7(4), 389-397, 2002
- 21 41. Olchev, A., Ibrom, A., Ross, T., Falk, U., Rakkibu, G., Radler, K., Grote, S., Kreilein, H., and
22 Gravenhorst G.: A modelling approach for simulation of water and carbon dioxide exchange
23 between multi-species tropical rain forest and the atmosphere. *J. Ecological Modelling*, 212,
24 122–130, 2008
- 25 42. Panferov, O., Ibrom, I., Kreilein, H., Oltchev, A., Rauf, A., June, T., Gravenhorst, G. and
26 Knohl, A.: Between deforestation and climate impact: the Bariri Flux tower site in the primary
27 montane rainforest of Central Sulawesi, Indonesia. *The Newsletter of FLUXNET* 2(3), 17-19,
28 2009
- 29 43. Phillips, O.L., Aragao, L., Lewis, S.L., Fisher, J.B., Lloyd, J., Lopez-Gonzalez, G., Malhi, Y.,
30 Monteagudo, A., Peacock, J., Quesada, C.A., van der Heijden, G., Almeida, S., Amaral, I.,
31 Arroyo, L., Aymard, G., Baker, T.R., Banki, O., Blanc, L., Bonal, D., Brando, P., Chave, J., de
32 Oliveira, A.C.A., Cardozo, N.D., Czimczik, C.I, Feldpausch, T.R., Freitas, M.A., Gloor, E.,
33 Higuchi, N., Jimenez, E., Lloyd, G., Meir, P., Mendoza, C., Morel, A., Neill, D.A., Nepstad,
34 D., Patino, S., Penuela, M.C., Prieto, A., Ramirez, F., Schwarz, M., Silva, J., Silveira, M.,
35 Thomas, A.S., ter Steege, H., Stropp, J., Vasquez, R., Zelazowski, P., Davila, E.A., Andelman,

- 1 S., Andrade, A., Chao, K.-J., Erwin, T., Di Fiore, A., Honorio, C. E., Keeling, H., Killeen, T.J.,
2 Laurance, W.F., Cruz, A.P., Pitman, N.C.A., Vargas, P.N., Ramirez-Angulo, H., Rudas, A.,
3 Salamao, R., Silva, N., Terborgh, J. and Torres-Lezama, A.: Drought sensitivity of the Amazon
4 rainforest. *Science* 323, 1344-1347, 2009
- 5 44. Propastin, P., Ibrom, A., Erasmi, S. and Knohl, A.: Effects of canopy photosynthesis saturation
6 on the estimation of gross primary productivity from MODIS data in a tropical forest. *Remote*
7 *Sensing of Environment* 121, 252–260, 2012
- 8 45. Setoh, T., Imawaki, S., Ostrovskii, A. and Umatani S.: Interdecadal Variations of ENSO
9 Signals and Annual Cycles Revealed by Wavelet Analysis. *Journal of Oceanography*, 55, 385-
10 394, 1999
- 11 46. Priestley, C.H.B., and Taylor, R.J.: On the assessment of surface heat flux and evaporation
12 using large-scale parameters. *Monthly Weather Review*, 100 (2), 81-92, 1972
- 13 47. Rasmusson, E.M., and Carpenter, T.H.: Variations in tropical sea surface temperature and
14 surface wind fields associated with the Southern Oscillation/ El Niño. *Monthly Weather*
15 *Review*, 110, 354-384, 1982
- 16 48. Rayner, P. J., and Law, R. M.: The relationship between tropical CO₂ fluxes and the El Niño-
17 Southern Oscillation, *Geophys. Res. Lett.*, 26(4), 493–496, doi:10.1029/1999GL900008, 1999
- 18 49. Reichstein, M., Bahn, M., Ciais, P., Frank, D., Mahecha, M.D., Seneviratne, S.I., Zscheischler,
19 J., Beer, C., Buchmann, N., Frank, D.C., Papale, D., Rammig, A., Smith, P., Thonicke, K., van
20 der Velde, M., Vicca, S., Walz, A., Wattenbach, M.: Climate extremes and the carbon cycle.
21 *Nature*, 500, 287- 295, 2013
- 22 50. Reverter, B.R., Carrara, A., Fernández, A., Gimeno, C., Sanz, M.J., Serrano-Ortiz, P., Sánchez-
23 Cañete, E.P., Were, A., Domingo, F., Resco, V., Burba, G.G., Kowalski, A.S.: Adjustment of
24 annual NEE and ET for the open-path IRGA self-heating correction: Magnitude and
25 approximation over a range of climate. *Agricultural and Forest Meteorology*, 151(12), 1856-
26 1861, 2011
- 27 51. Saji, N. H., Goswami, B. N., Vinayachandran, P. N., Yamagata, T.: A dipole mode in the
28 tropical Indian Ocean. *Nature*, 401, 360-363, 1999
- 29 52. van Straaten, O., Veldkamp, E, Corre, M.D.: Simulated drought reduces soil CO₂ efflux and
30 production in a tropical forest in Sulawesi, Indonesia. *Ecosphere*, 2, art119, 2011
- 31 53. Wang, C.: Atmospheric circulation cells associated with the El Niño-Southern Oscillation. *J.*
32 *Climate*, 15, 399-419, 2002
- 33 54. Wheeler, M. C., and Kiladis, G. N.: Convectively coupled equatorial waves: Analysis of clouds
34 and temperature in the wavenumber–frequency domain. *J. Atmos. Sci.*, 56, 374–399, 1999.

- 1 55. Yeh, S.-W., Kug, J.-S., Dewitte, B., Kwon, M.-H., Kirtman, B., and Jin, F.-F.: El Niño in a
2 changing climate. *Nature*, 461, 511-514, 2009
- 3 56. Yuan, Y. and Yan H.: Different types of La Niña events and different responses of the tropical
4 atmosphere. *Chinese Science Bulletin* 58, 406-415, 2013
- 5 57. Zhang, C.: Madden-Julian Oscillation. *Reviews of Geophysics*, 43, RG2003, 2005, doi:
6 10.1029/2004RG000158.
- 7 58. Zhang, C., and Gottschalck, J.: SST Anomalies of ENSO and the Madden–Julian oscillation in
8 the equatorial Pacific. *J. Climate*, 15, 2429–2445, 2002
- 9

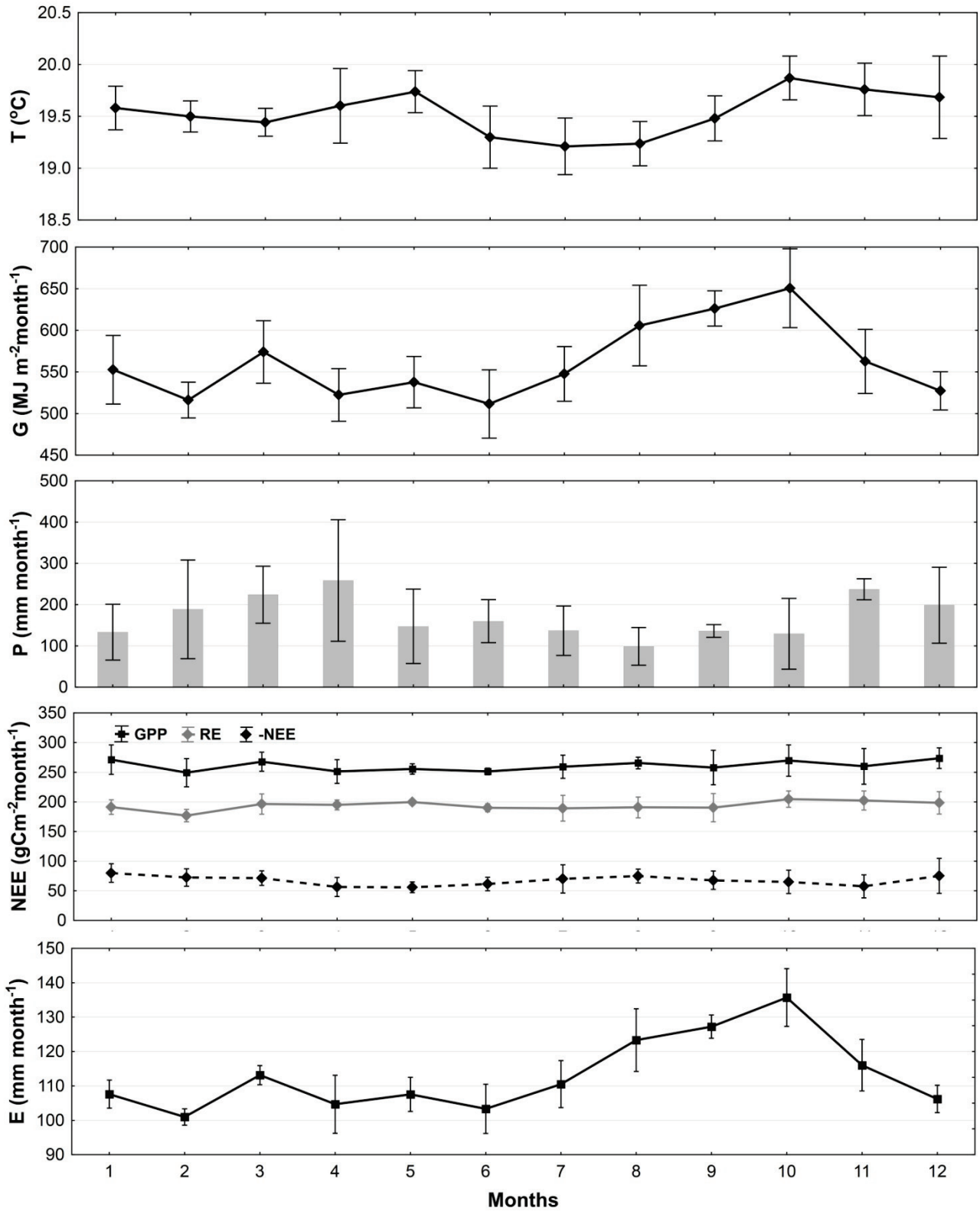
1
2



3
4
5
6
7

Figure 1. Geographical location of a study area (marked by black triangle) in tropical rain forest in Central Sulawesi (Indonesia) and Nino4 and Nino3.4 regions.

1

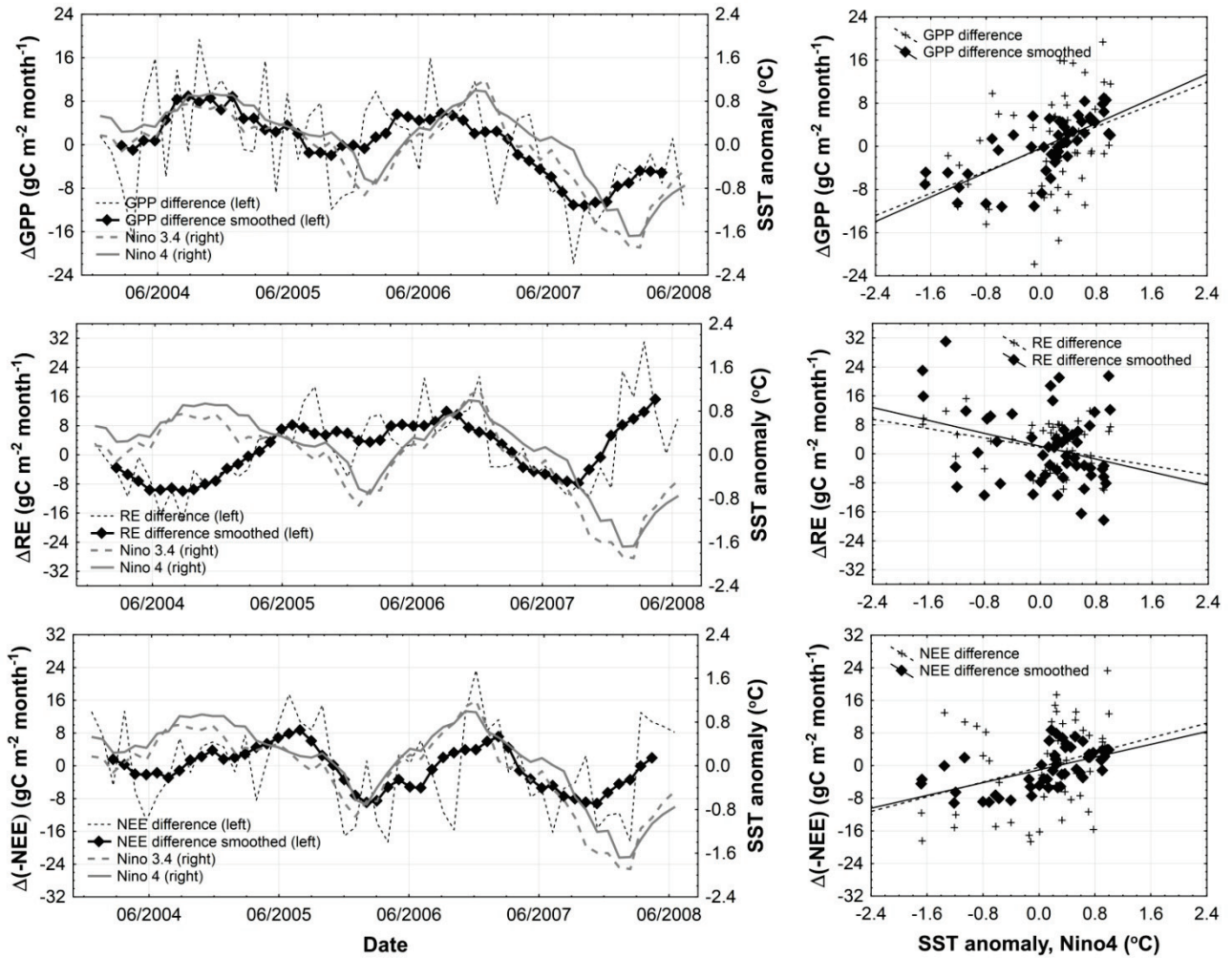


2

3 Figure 2. Mean intra-annual courses of air temperature (T), global solar radiation (G), precipitation
4 (P), NEE, GPP, RE and ET for the tropical rain forest in Bariri. Vertical whiskers indicate standard
5 deviations (SD).

6

1



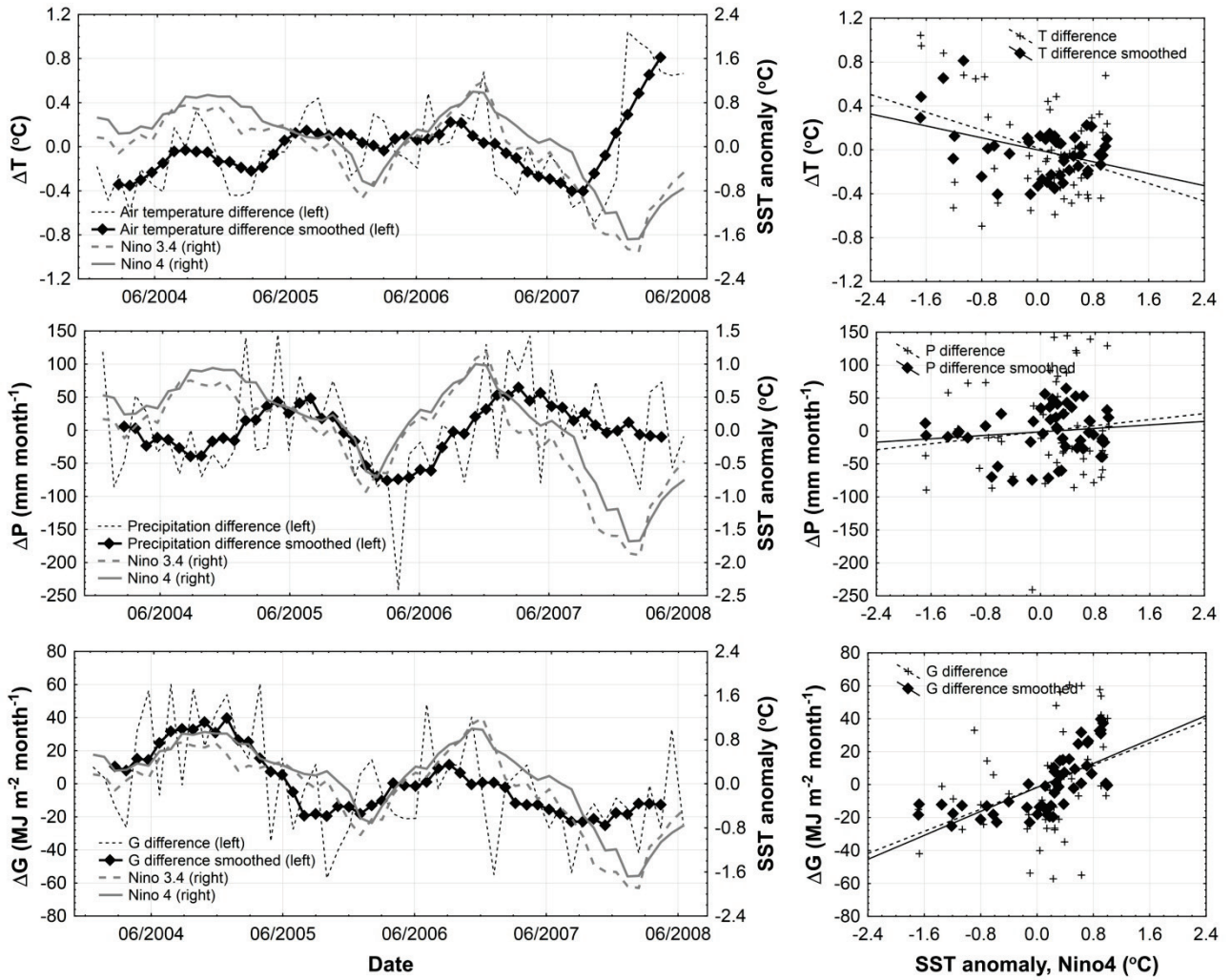
2

3 Figure 3. Comparisons of inter-annual pattern of SST anomalies in Nino4 and Nino3.4 zones of
4 equatorial Pacific with variability of both deviations and 7 month (± 3 months) moving average
5 deviations of monthly GPP, RE and NEE values from mean monthly values of GPP, RE and NEE
6 averaged over the entire measuring period from 2004 to 2008.

7

8

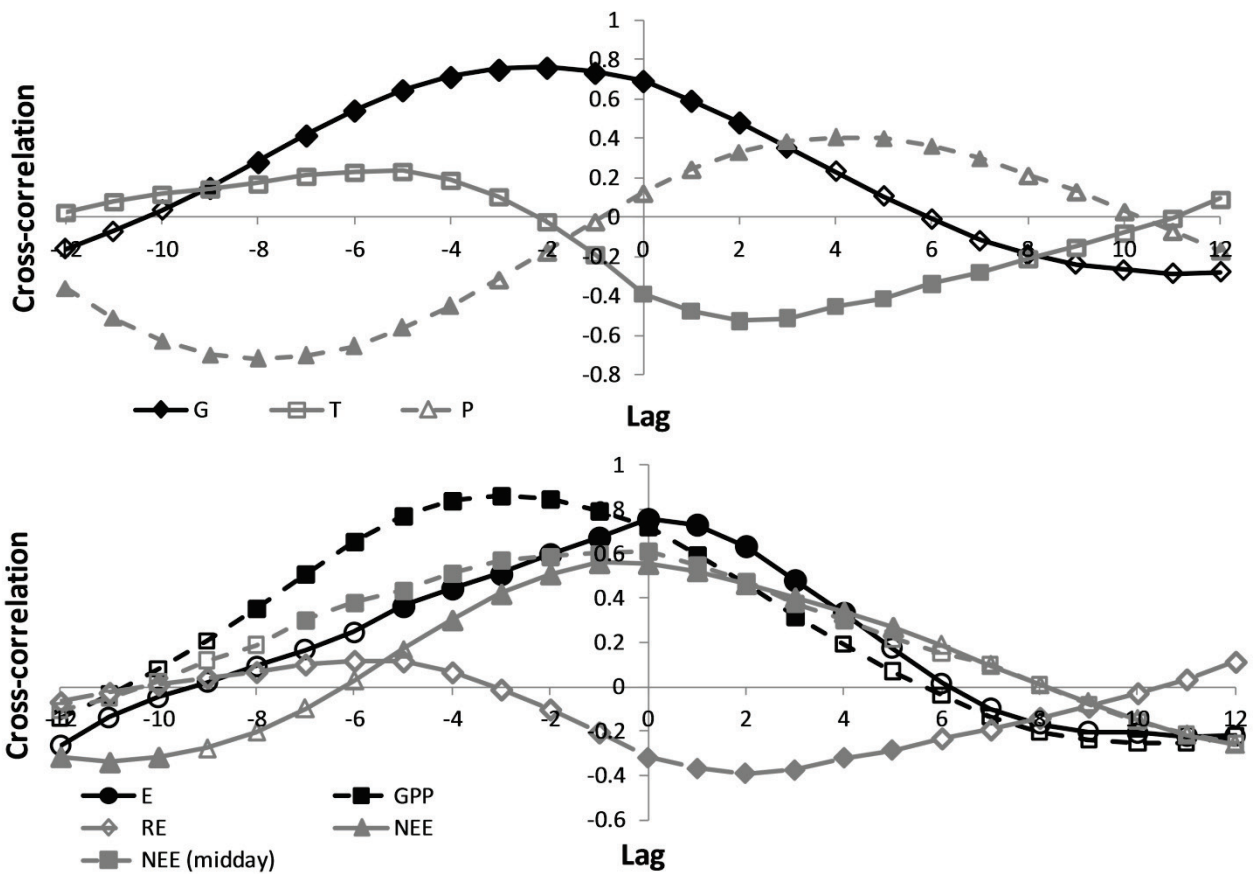
1



2

3 Figure 4. Comparisons of inter-annual pattern of SST anomalies in Nino4 and Nino3.4 zones of
4 equatorial Pacific with variability of both deviations and 7 month (± 3 months) moving average
5 deviations of monthly air temperature (T), precipitation (P) and global radiation (G) values from
6 mean monthly values of T, P and G averaged over the entire measuring period from 2004 to 2008.

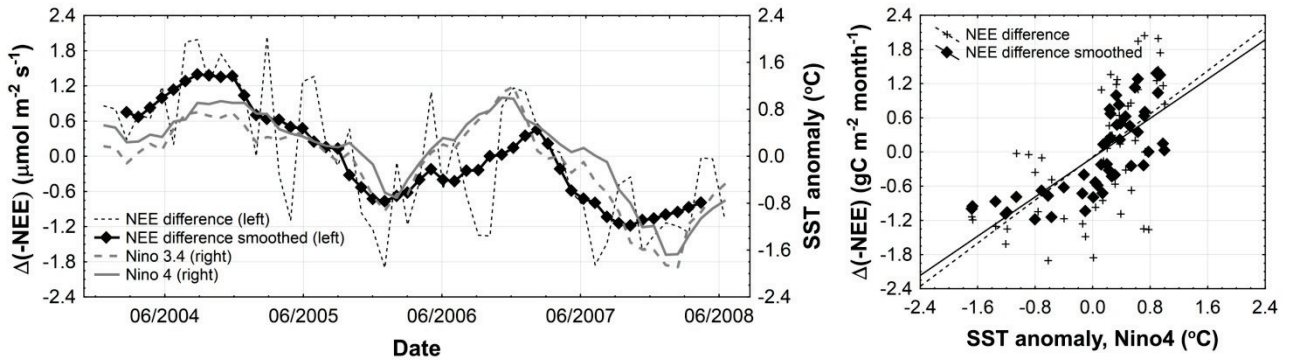
7



1
2
3
4
5
6
7
8

Figure 5. Cross-correlation functions between ΔG_{MA} , ΔT_{MA} , ΔP_{MA} , ΔE_{MA} , ΔGPP_{MA} , ΔRE_{MA} , ΔNEE_{MA} and midday ΔNEE_{MA} values and SST anomalies in Nino4 zone of equatorial Pacific. Filled symbols are corresponded to p-value < 0.05 and non-filled symbols - to p > 0.05. Lag step is 1 month.

1

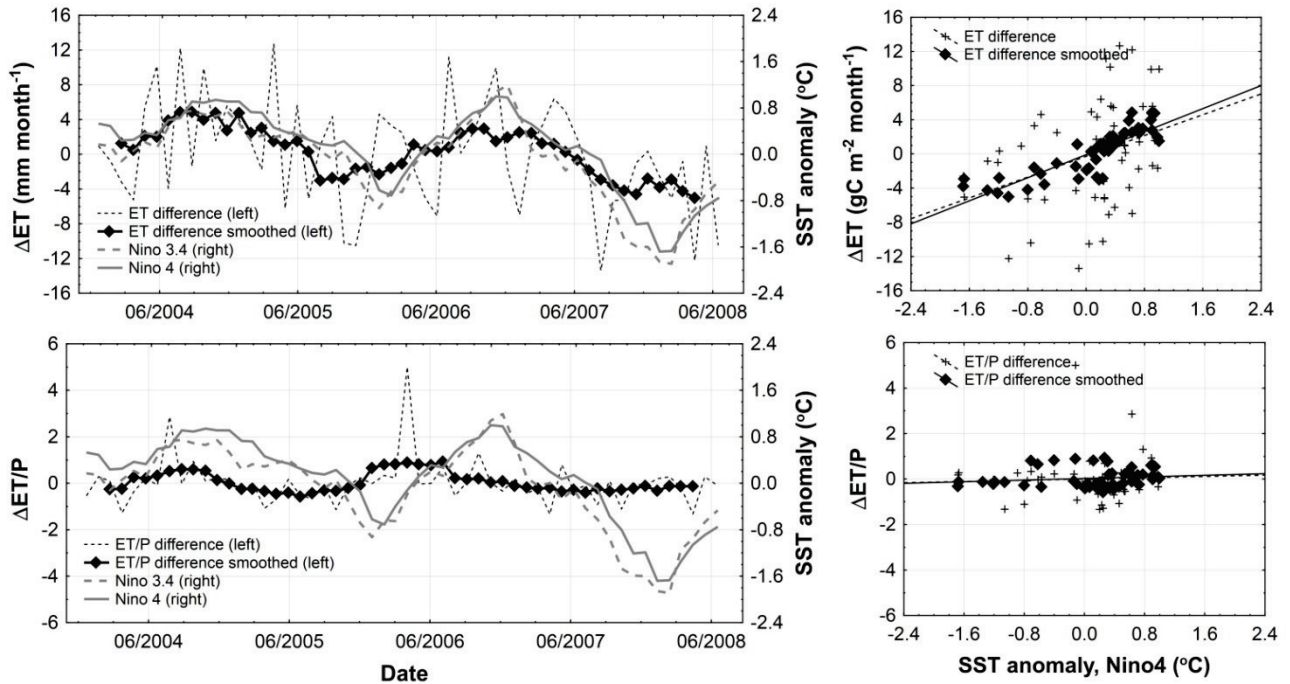


2

3 Figure 6. Comparisons of inter-annual pattern of SST anomalies in Nino4 and Nino3.4 zones of
4 equatorial Pacific with variability of both deviations and 7 month (± 3 months) moving average
5 deviations of midday NEE (10:00-14:00) values from mean monthly midday values of NEE
6 averaged over the entire measuring period from 2004 to 2008.

7

1



2

3

4 Figure 7. Comparisons of inter-annual pattern of SST anomalies in Nino4 and Nino3.4 zones of
5 equatorial Pacific with variability of both deviations and 7 month (± 3 months) moving average
6 deviations of monthly ET rate and ratio ET/P from mean monthly ET rate and ET/P averaged over
7 the entire measuring period from 2004 to 2008.

8

9